UDC 544.6.018.2

R.A. Panteleimonov, O.V. Boichuk, K.D. Pershina, V.M. Ogenko

STRUCTURAL AND ELECTROCHEMICAL PROPERTIES OF N-DOPED GRAPHENE–GRAPHITE COMPOSITES

V.I. Vernadsky Institute of General and Inorganic Chemistry of the National Academy of Sciences of Ukraine, Kyiv, Ukraine

This work studied the impact of graphene content and heat treatment on the structural changes and electrical parameters of graphite/N-doped graphene mixtures. Using photoelectron spectroscopy the appearance of two types of carbon-containing phases was detected in the visible range of the N-doped graphene samples synthesized from liquid nitrogen. The following features of the samples were shown: one typical structure of graphene ($sp^2C–sp^2C$), two atypical structures ($sp^3C–N$ and the C–O bond), and graphene components modified with nitrogen (pyridine–N, pyrrole–N, graphite–N and oxidized N–O). The dependence between the ratio of components in graphite–graphene mixtures and their electrochemical properties was found. The effect of graphite content and heat treatment on the change in the type of conductivity in a graphite–graphene mixture was determined by comparison of resistance and capacitance distribution in the frequency range of 100–900 Hz. The change of the graphite concentration in the graphene–graphite mixture allows governing the type of doping and electrical parameters of the mixtures.

Keywords: graphene, graphite, capacity, electrical conductivity, synthesis, liquid nitrogen.

DOI: 10.32434/0321-4095-2022-145-6-61-67

Introduction

The graphene-based supercapacitor is one of the most discussed topics in the scientific community today. They have the ability to a formation such structures as carbon nanotubes, based on graphene sheets rolled into a tube with a diameter in the range of 1 nm to 100 nm [1]. The specific surface area of carbon nanotubes can vary in the range of 300 to 400 m^2/g. The specific surface area of many graphenes under alternating current (AC) increases by 3–8 times and is approximately 1000–3000 m^2/g due to the entire surface of carbon nanotubes being available for ions [2,3]. Therefore, such properties of graphene as a new carbon nanostructure have promoted scientists from different countries to produce new electrochemical two-layer capacitors [4,5]. In 2006, Ruoff et al. [6] used chemically modified graphene to obtain a capacity of 130 F/g. In 2010, electrodes made from a mixture of carbon nanotubes and graphene flakes were investigated [7]. Capacitors made from these electrodes showed a capacity of 290 F/g and 200 F/g in aqueous and organic electrolytes, respectively. These values were 20% higher than for graphene-based electrodes without modification. This was explained by the fact that graphene alone is capable of repackaging with the formation of graphite and nanotubes due to van der Waals forces from beams, reducing the active surface area. A composite of these structures, on the contrary, prevents repackaging ability and the formation of beams in the entire graphene structure, thereby increasing the active surface area, which accelerates the diffusion of ions [8].

In the graphene/graphite composite with nitrogen admixture, the graphite particles are dispersed in a three-dimensional graphene framework with a large number of open pores. These pores in the graphene framework act as connectors of graphite particles and improve ions transfer. The graphene framework also acts as an expansion absorber in the anodes of the lithium-ion battery, reducing large voltages that can occur at high discharge rates. As a

result, the nitrogen-doped graphene/graphite mixture provides excellent electrochemical characteristics for the lithium-ion battery, such as a high specific capacity of up to 781 mA·h/g, a bandwidth of 351 mA·h/g, and rather interesting stability: maintaining a capacity of 98.1% at 10^0C after 1000 cycles [9]. A challenge, however, will remain for facile integration of graphene into electronic devices: control over the deposition of graphene nanostructures (GNRs), control on the atomic edge arrangements, and creating efficient electrical contacts [10]. In many cases, graphite is used as an electroconductive impurity for these purposes [11]. Graphite is an infinite three-dimensional crystal complicated of stacked layers consisting of sp^2 hybridized carbon atoms. In 3D graphite crystals, the layers interact weakly through van der Waals forces. In the presence of graphite with sp^2 hybridized carbon atoms, often infinite graphene crystals become finite, surface and boundaries appear, forming non-three coordinated atoms at the edges, and if the size is in the order of nanometers, we have a graphitic nanostructure (GN) that exhibits different properties from those observed in pure graphite. As the number of graphene layers increases, the band structure becomes more complicated: several charge carriers appear [10,12], and the conduction and valence bands start notably overlapping. On the other hand, it was found that the N-doped-graphene-like material exhibited an n-type semiconducting behavior, and contained between 2 and 6 layers with a variable N concentration (i.e. 1.2–8.9 at.%), depending on the NH_3 flow rate used in the CVD process. Subsequently, graphene nanoribbons doped with nitrogen via Joule heating in the presence of NH_3 were produced [10]. It was theoretically found that the presence of C–O bonds on edges resulted in p-doped carbon nanoribbons [10]. Thus, the presence of a 3D structure with free sp^2 hybridized atoms of C in graphite could regulate electrical properties and types of the semiconducting conductivity of the graphite–N-doped graphene composites.

Therefore, our study was aimed to establish the effects of graphene content and heat treatment on the structural changes and electrical parameters (conductivity and capacity) of graphite–N-doped graphene mixture in which graphene was from liquid nitrogen.

Experimental

Electrolytic graphite and graphene synthesized in a plasma-arc discharge in liquid nitrogen were used as starting components. To prepare samples, nitrogen residues were evaporated at room temperature of 20^0C. The fabricated graphene was mechanically transferred to a closed container.

Then, graphene and graphite were mixed according to ratios given in Table 1. Acrylic glue (5 wt.%) with impurities of dimethylformamide was used as a plasticizer of the active mass to reduce the viscosity of the plasticizer (10 wt.%). Next, the samples were pressed on a press Dezimalpresse DP 36 with a maximum pressure of 50 N in a round mold with a diameter of 2 cm.

Heat treatment of the samples was performed in an oven SNOL 67/350 for 1 h with a gradual increase in the temperature to 250^0C.

Table 1

Composition and processing conditions of graphite–graphene mixtures

No.	Sample	Mass ratios of graphene/graphite	Note
1	Synthesized graphene in a nitrogen medium	1/5.26	
2		1/3	
3		1/1	
4		1/1	treatment at 250^0C

The electronic structure of the internal C1s and N1s levels of the synthesized nanostructures was studied by X-ray photoelectron spectroscopy. The electronic surface structure of graphene-like nanoparticles was investigated on an electronic spectrometer EC-2402UM (E MgK*=1253.6 eV, P=300 W), the depth of analysis was 2–3 nm, and the vacuum in the measurement chamber was 10^{-7} Pa. Calibration of the spectra was performed along the C1s line (E_b=285.0 eV). The RFS spectra of the C1s and N1s levels were decomposed into components by the Gauss-Newton method. The intensity of the components and their binding energy varied. The total width of the components ΔE=1.4 eV and the Gauss-Lorentz contribution ratio G/L=0.7 during the spectrum decomposition were fixed. During decomposition, the intensity of the components and their binding energy varied. Samples were prepared in the form of thin films on an aluminum substrate (10×10 mm) by evaporation of the alcohol suspension.

EIS measurements were performed on an electrochemical module Autolab 30 PGSTAT301N MetrohmAutolab in a two-electrode cell (disk cell) in the frequency range of 10^{-2} to 10^3 Hz. The results were processed using ZView2 software.

The following equations were used to calculate the capacity and obtain charge distribution map:

$$X_C = \frac{1}{\omega C}, \quad (1)$$

$$Z = \sqrt{R^2 + \left(X_L - X_C\right)^2}, \quad (2)$$

$$Z = R, \quad (3)$$

where X_C is the resistance of the capacitor; and X_L is the resistance of the inductor.

At X_L=0, we have:

$$Z = \sqrt{R^2 + X_C^2}, \quad (4)$$

$$\sqrt{R^2 - X_C^2} = \frac{1}{\omega C}, \quad (5)$$

$$C = \frac{1}{\omega\sqrt{R^2 + X_C^2}}. \quad (6)$$

Results and discussion

The appearance of carbon-containing phases of the graphene samples without nitrogen and with nitrogen in the visible range of the photoelectron spectrum was fixed by the XPS analysis. Gauss-Newton method showed that C1s-line decomposed into a few components (Figs. 1 and 2) next to the bond sp^2C-sp^2C (E_b=284.8 eV) that is typical of graphene. It was detected the binding of the component with E_b=286.4 eV with two links such as the nitrogen-mods field graphene bond sp^3C-N and the C–O bond [12]. The presence of the C1s-line in the energy area with E_b=287.3 eV applies to the C=O bond, which is missing in the C1s spectrum in the optical range of the transparent phase.

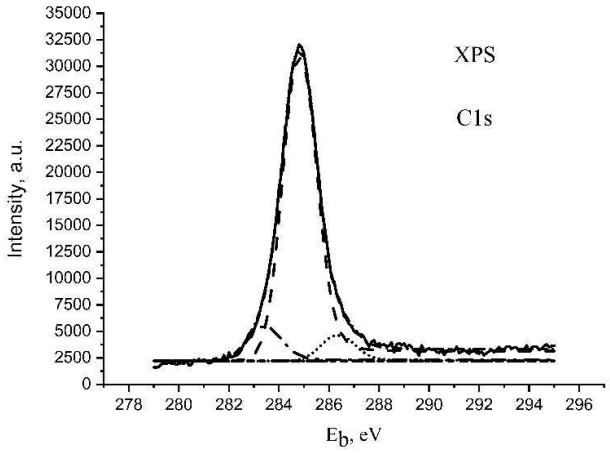

Fig. 1. The photoemission response of carbon phase without nitrogen. SWCNTs were measured with a 400 eV photon excitation. E_b is the binding energy

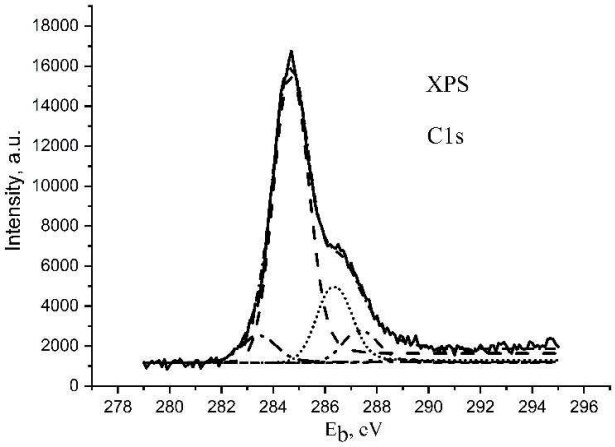

Fig. 2. The photoemission response of carbon phase with nitrogen

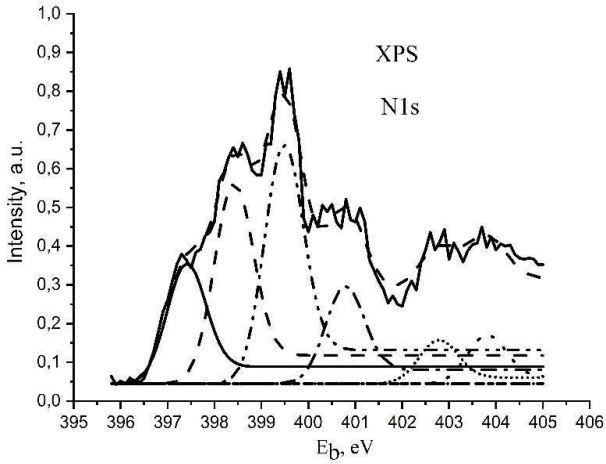

Fig. 3. The photoemission response of nitrogen phase

Depending on the local configuration, the different chemical shifts are seen in the N1s spectrum. Thus, there are typical nitrogen modified graphene components on the N1s-bands (Figs. 3 and 4) with E_b=398.4 eV (pyridine–N), E_b=400.0 eV (pyrrole–N), E_b=401.6 eV (graphite–N), and E_b=402.7 eV (oxidized N–O) [12]. The component in the area of 398.4 eV can also be assigned to the nitrile-N group, where nitrogen is covalently linked to a carbon atom and two hydrogen atoms. The component that belongs to pyrrole–N can also be a substitution of N in the stone-wales defect or part of the amine, pyridine, nitroso, or cyan group [13]. All detected components are summarized in Table 2.

Calculations of the average electrical conductivity data in systems with graphene synthesized in a nitrogen medium show the dependence of the increase of the electrical

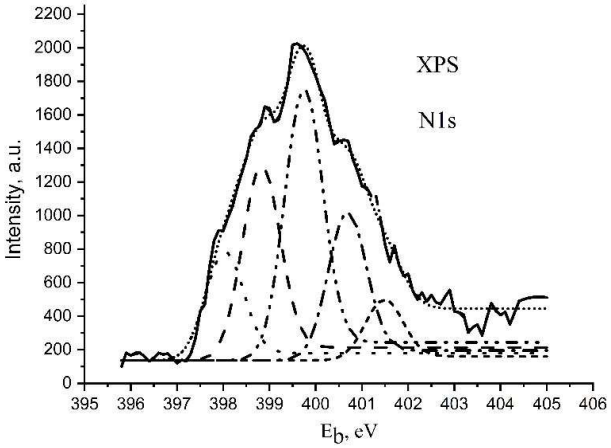

Fig. 4. The photoemission response of nitrogen phase

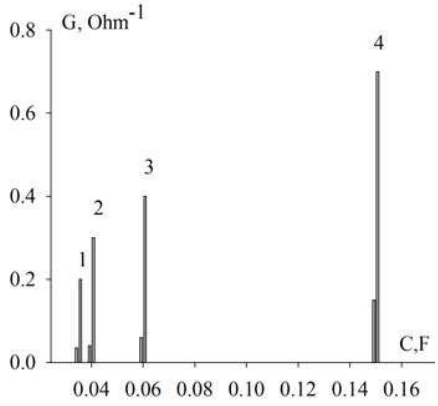

Fig. 5. Comparison of the average conductivity and capacity between the samples (numbering is given according to Table 1)

Table 2

Results of photoemission measurements

Materials	max C1s, eV	max N1s, eV	G/L, eV
graphite	284.4	–	0.16–0.18
graphene	284.8	–	0.529
graphene–N	286.4	–	0.37
graphite–N	–	401.6	0.83
pyridine–N	–	398.4	0.42
pyrrole–N	–	400	0.43

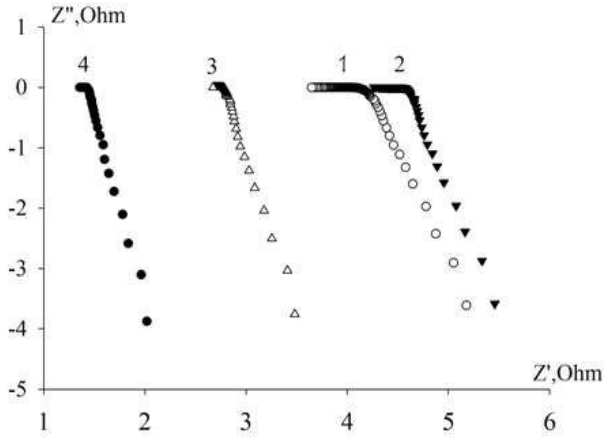

Fig. 6. EIS data of the samples (numbering is given according to Table 1)

conductivity and an increase of the capacitance on the graphene content (Fig. 5). Increasing the graphene content leads to an increase in the capacity and the electrical conductivity of the mixture, which indicates an increase in the electron's mobility [10,11]. High values of capacitance and conductivity were obtained in the systems with a ratio of graphene/graphite=1:1 (samples 3 and 4). However, the maximum average values of capacity (almost 2 times higher) are observed in the system with equal content of graphene and graphite, which is synthesized in nitrogen with heat treatment of the sample at 250^{0}C. Further analysis of the impedance spectra of these samples detected the absence of the visible impact of the graphite content on the Z'' data. (Fig. 6). However, the graphical integration of the active resistance and capacity data on the frequency plane [14,15] showed the changes in the charges distribution in the samples in various frequency ranges (Fig 7).

For the samples 1 and 2 with high content of graphite (Fig. 7,a,b) at the frequency less than 200 Hz, an increase in the active resistances was detected which is connected with a high density of charges. In the frequency range more than 200 Hz, low resistance was observed in a narrow region. Such dependence of the resistance (conductivity) is characteristic of p-type semiconductors [15]. Pyridine–N and pyrrole–N have electron acceptor atoms that formed the positive vacancies. Therefore, the pyridine nitrogen at high concentration of graphite takes part in the formation of an extrinsic p-type semiconductor.

For samples 3 and 4 with graphene/graphite content=1:1, the dependence between resistance and frequency has an opposite nature. At the frequencies less than 200 Hz, a decrease in the active resistances was detected, while in the frequency range more than 200 Hz the presence of narrow high resistance region was observed. Such behavior looks like the behavior of pure graphite, and nitrogen-substituted graphene (graphene–N) with an sp^3C–N bond. In such a case, the decrease in the graphite content increases the part of electron's donors and changes the semiconductor configuration into n-type doping. Thermal treatment of sample stabilizes such type of

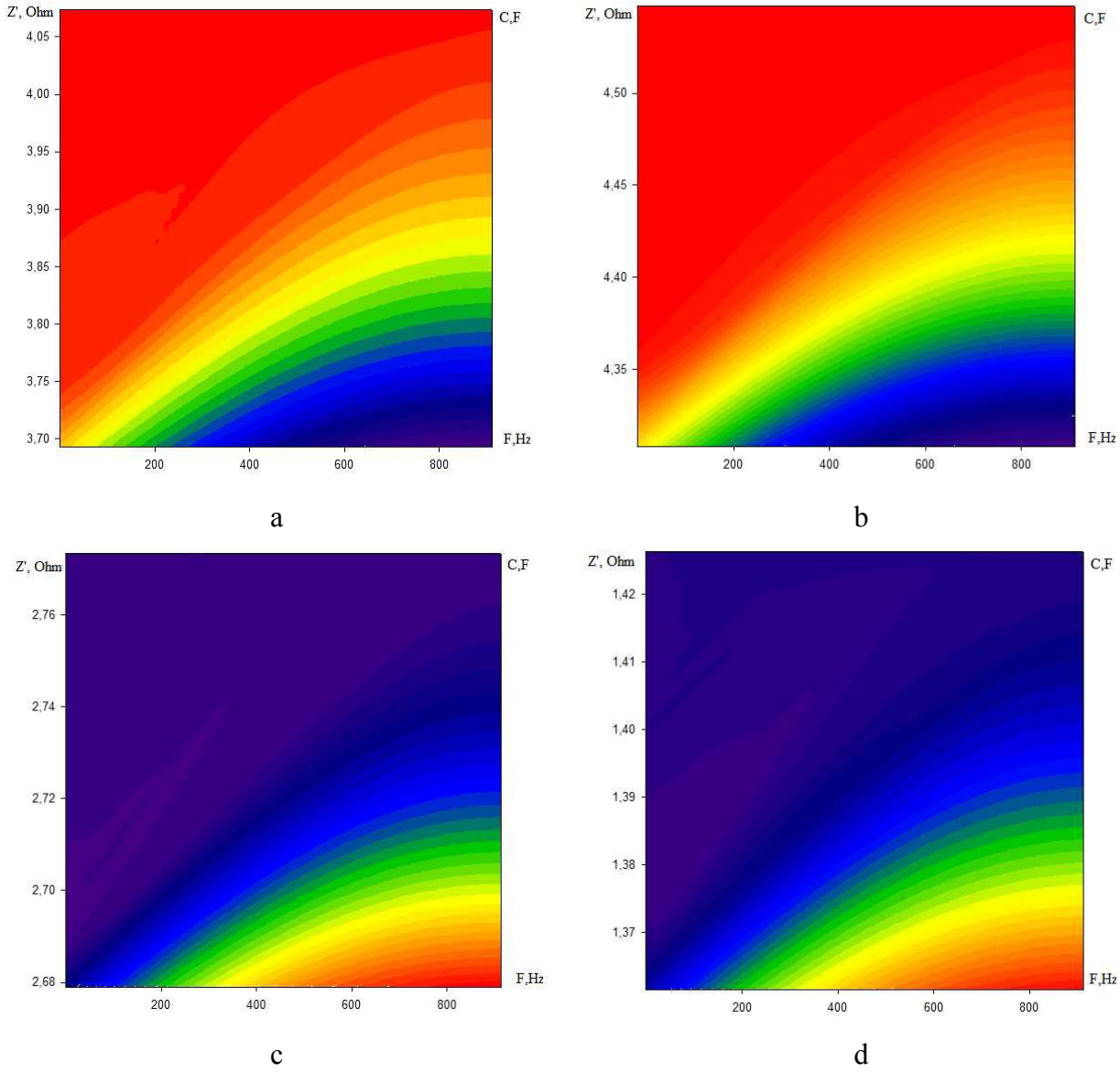

Fig 7. Maps of charges distribution in the samples: a – 1, b – 2, c – 3, d – 4 (numbering is given according to Table 1)

doping. So, due to change of the graphite concentration in the graphene/graphite mixtures, there is the ability to regulate both the type of doping and electrical parameters.

Conclusions

The electrical parameters of graphite–graphene systems with different mass concentrations of graphene synthesized from liquid nitrogen were investigated by photoelectron spectroscopy and impedance spectroscopy. Photoelectron spectroscopy revealed the following: the one typical of graphene structure (sp^2C-sp^2C), two atypical structures (sp^3C-N and the C–O bond), and typical nitrogen modified graphene components (pyridine–N, pyrrole–N, graphite–N and oxidized N–O). The dependence between graphite-graphene ratio and electrochemical properties was established. In the samples with high content of graphite, the pyridine nitrogen takes part in the formation of an extrinsic p-type semiconductor. In the samples with graphene/graphite content=1:1, the share of donors of electrons increases and the semiconductor configuration changes into n-type doping. Thermal treatment of sample stabilizes such type of doping. The change of the graphite concentration in the graphene/graphite mixture allows regulating both the type of doping and electrical parameters of the mixture.

REFERENCES

1. *High* power electrochemical capacitors based on carbon nanotube electrodes / Niu C., Sichel E.K., Hoch R., Moy D., Tennent H. // Appl. Phys. Lett. – 1997. – Vol.70. – No. 11. – P.1480-1482.

2. *Flexible* energy storage devices based on nanocomposite paper / Pushparaj V.L., Shaijumon M.M., Kumar A., Murugesan S., Ci L., Vajtai R., Ajayan P.M. // Proc. Nat. Acad. Sci. – 2007. – Vol.104. – No. 34. – P.13574-13577.

3. *Printable* thin film supercapacitors using single-walled carbon nanotubes / Kaempgen M., Chan C.K., Ma J., Cui Y., Gruner G. // Nano Lett. – 2009. – Vol.9. – No. 5. – P.1872-1876.

4. *Hu L., Wu H., Cui Y.* Printed energy storage devices by integration of electrodes and separators into single sheets of paper // Appl. Phys. Lett. – 2010. – Vol.96. – No. 18. – Art. No. 183502.

5. *Highly* conductive paper for energy-storage devices / Hu L., Choi J.W., Yang Y., Jeong S., La Mantia F., Cui L.F., Cui Y. // Proc. Nat. Acad. Sci. – 2009. – Vol.106. – No. 51. – P.21490-21494.

6. *Graphene-based* ultracapacitors / Stoller M.D., Park S., Zhu Y., An J., Ruoff R.S. // Nano Lett. – 2008. – Vol.8. – No. 10. – P.3498-3502.

7. *Graphene* and carbon nanotube composite electrodes for supercapacitors with ultra-high energy density / Cheng Q., Tang J., Ma J., Zhang H., Shinya N., Qin L.C. // Phys. Chem. Chem. Phys. – 2011. – Vol.13. – No. 39. – P.17615-17624.

8. *High power* graphene–carbon nanotube hybrid supercapacitors / Ansaldo A., Bondavalli P., Bellani S., Del Rio Castillo A. E., Prato M., Pellegrini V., Bonaccorso, F. // ChemNanoMat. – 2017. – Vol.3. – No. 6. – P.436-446.

9. *N-doped* graphene/graphite composite as a conductive agent-free anode material for lithium ion batteries with greatly enhanced electrochemical performance / Guanghui W., Ruiyi L., Zaijun L., Junkang L., Zhiguo G., Guangli W. // Electrochim. Acta. – 2015. – Vol.171. – P.156-164.

10. *Graphene* and graphite nanoribbons: morphology, properties, synthesis, defects and applications / Terrones M., Botello-Mendez A.R., Campos-Delgado J., Lopez-Urias F., Vega-Cantu Y.I., Rodriguez-Macias F.J., Terrones H. // Nano Today. – 2010. – Vol.5. – No. 4. – P.351-372.

11. *Graphene* oxide/carbon nanoparticle thin film based IR detector: surface properties and device characterization / Chowdhury F.A., Hossain M.A., Uchida K., Tamura T., Sugawa K., Mochida T., Alam M.S. // AIP Adv. – 2015. – Vol.5. – No. 10. – Art. No. 107228.

12. *Connecting* dopant bond type with electronic structure in N-doped graphene / Schiros T., Nordlund D., Pamlovam L., Prezzi D., Zhao L., Kim K.S., Pasupathy A.N. // Nano Lett. – 2012. – Vol.12. – No.8. – P.4025-4031.

13. *X-ray* photoelectron spectroscopy of graphitic carbon nanomaterials doped with heteroatoms / Susi T., Pichler T., Ayala P. // Beilstein J. Nanotechnol. – 2015. – Vol.6. – No. 1. – P.177-192.

14. *Control* of the state of primary alkaline Zn–MnO_2 cells using the electrochemical impedance spectroscopy method / Riabokin O.L., Boichuk A.V., Pershina K.D. // Surf. Eng. Appl. Electrochem. – 2018. – Vol.54. – P.614-622.

15. *Thermo-galvanic* effects in a non-isothermal element based on the of iron-carbon compositional electrode and alkaline electrolyte / Boichuk O., Pershina K., Riabokin O., Kravchenko A., Panteleimonov R. // Ukr. Chem. J. – 2020. – Vol.86. – No. 4. – P.108-117.

Received 19.01.2022

СТРУКТУРНІ ТА ЕЛЕКТРОХІМІЧНІ ВЛАСТИВОСТІ N-ЛЕГОВАНИХ ГРАФЕН–ГРАФІТОВИХ КОМПОЗИТІВ

Р.А. Пантелеймонов, О.В. Бойчук, К.Д. Першина, В.М. Огенко

Досліджено вплив вмісту графену та термічного оброблення на структурні зміни та електричні параметри суміші графіт/N-легований графен. Методом фотоелектронної спектроскопії зафіксовано появу вуглецьвмісних фаз без азоту та з азотом у видимому діапазоні зразків N-легованого графену, синтезованих із рідкого азоту. Виявлено: типову для структури графену ($sp^2C–sp^2C$), дві нетипові структури ($sp^3C–N$ і зв'язок CO) і типові компоненти графену, модифіковані азотом (піридин–N, пірол–N, графіт–N та окислений N–O). Встановлено залежність між співвідношенням графіт-графен та електрохімічними властивостями. Порівнянням розподілу опору та ємності в діапазоні частот 100–900 Гц у графіт-графеновій суміші визначено вплив вмісту графіту та термічного оброблення на зміну типу провідності. Зміна концентрації графіту в суміші графен-графіт дає можливість регулювати тип легування та електричні параметри суміші.

Ключові слова: графен, графіт, ємність,

електропровідність, синтез, рідкий азот.

STRUCTURAL AND ELECTROCHEMICAL PROPERTIES OF N-DOPED GRAPHENE–GRAPHITE COMPOSITES

R.A. Panteleimonov* *, O.V. Boichuk, K.D. Pershina, V.M. Ogenko

V.I. Vernadsky Institute of General and Inorganic Chemistry of the National Academy of Sciences of Ukraine, Kyiv, Ukraine

*** e-mail: radik20031@gmail.com**

This work studied the impact of graphene content and heat treatment on the structural changes and electrical parameters of graphite/N-doped graphene mixtures. Using photoelectron spectroscopy the appearance of two types of carbon-containing phases was detected in the visible range of the N-doped graphene samples synthesized from liquid nitrogen. The following features of the samples were shown: one typical structure of graphene ($sp^2C–sp^2C$), two atypical structures ($sp^3C–N$ and the C–O bond), and graphene components modified with nitrogen (pyridine–N, pyrrole–N, graphite–N and oxidized N–O). The dependence between the ratio of components in graphite–graphene mixtures and their electrochemical properties was found. The effect of graphite content and heat treatment on the change in the type of conductivity in a graphite–graphene mixture was determined by comparison of resistance and capacitance distribution in the frequency range of 100–900 Hz. The change of the graphite concentration in the graphene–graphite mixture allows governing the type of doping and electrical parameters of the mixtures.

Keywords: graphene; graphite; capacity; electrical conductivity; synthesis; liquid nitrogen.

REFERENCES

1. Niu C, Sichel EK, Hoch R, Moy D, Tennent H. High power electrochemical capacitors based on carbon nanotube electrodes. *Appl Phys Lett.* 1997; 70: 1480-1482. doi: 10.1063/1.118568.

2. Pushparaj VL, Shaijumon MM, Kumar A, Murugesan S, Ci L, Vajtai R, et al. Flexible energy storage devices based on nanocomposite paper. *Proc Natl Acad Sci USA.* 2007; 104(34): 13574-13577. doi: 10.1073/pnas.0706508104.

3. Kaempgen M, Chan CK, Ma J, Cui Y, Gruner G. Printable thin film supercapacitors using single-walled carbon nanotubes. *Nano Lett.* 2009; 9(5): 1872-1876. doi: 10.1021/nl8038579.

4. Hu L, Wu H, Cui Y. Printed energy storage devices by integration of electrodes and separators into single sheets of paper. *Appl Phys Lett.* 2010; 96: 183502. doi: 10.1063/1.3425767.

5. Hu L, Choi JW, Yang Y, Jeong S, La Mantia F, Cui LF, et al. Highly conductive paper for energy-storage devices. *Proc Natl Acad Sci USA.* 2009; 106(51): 21490-21494. doi: 10.1073/pnas.0908858106.

6. Stoller MD, Park S, Zhu Y, An J, Ruoff RS. Graphene-based ultracapacitors. *Nano Lett.* 2008; 8(10): 3498-3502. doi: 10.1021/nl802558y.

7. Cheng Q, Tang J, Ma J, Zhang H, Shinya N, Qin LC. Graphene and carbon nanotube composite electrodes for supercapacitors with ultra-high energy density. *Phys Chem Chem Phys.* 2011; 13: 17615-17624. doi: 10.1039/C1CP21910C.

8. Ansaldo A, Bondavalli P, Bellani S, Del Rio Castillo AE, Prato M, Pellegrini V, et al. High power graphene–carbon nanotube hybrid supercapacitors. *ChemNanoMat.* 2017; 3: 436-446. doi: 10.1002/cnma.201700093.

9. Guanghui W, Ruiyi L, Zaijun L, Junkang L, Zhiguo G, Guangli W. N-doped graphene/graphite composite as a conductive agent-free anode material for lithium ion batteries with greatly enhanced electrochemical performance. *Electrochim Acta.* 2015; 171: 156-164. doi: 10.1016/j.electacta.2015.05.016.

10. Terrones M, Botello-Mendez AR, Campos-Delgado J, Lopez-Urias F, Vega-Cantu YI, Rodriguez-Macias FJ, et al. Graphene and graphite nanoribbons: morphology, properties, synthesis, defects and applications. *Nano Today.* 2010; 5(4): 351-372. doi: 10.1016/j.nantod.2010.06.010.

11. Chowdhury FA, Hossain MA, Uchida K, Tamura T, Sugawa K, Mochida T, et al. Graphene oxide/carbon nanoparticle thin film based IR detector: surface properties and device characterization. *AIP Adv.* 2015; 5(10): 107228. doi: 10.1063/1.4935042.

12. Schiros T, Nordlund D, Palova L, Prezzi D, Zhao L, Kim KS, et al. Connecting dopant bond type with electronic structure in N-doped graphene. *Nano Lett.* 2012; 12(8): 4025-4031. doi: 10.1021/nl301409h.

13. Susi T, Pichler T, Ayala P. X-ray photoelectron spectroscopy of graphitic carbon nanomaterials doped with heteroatoms. *Beilstein J Nanotechnol.* 2015; 6(1): 177-192. doi: 10.3762/bjnano.6.17.

14. Riabokin OL, Boichuk AV, Pershina KD. Control of the state of primary alkaline $Zn–MnO_2$ cells using the electrochemical impedance spectroscopy method. *Surf Eng Appl Electrochem.* 2018; 54: 614-622. doi: 10.3103/S1068375518060108.

15. Boichuk O, Pershina K, Riabokin O, Kravchenko A, Panteleimonov R. Thermo-galvanic effects in a non-isothermal element based on the of iron-carbon compositional electrode and alkaline electrolyte. *Ukr Chem J.* 2020; 86(4): 108-117. doi: 10.33609/2708-129X.86.4.2020.108-117.